JOURNAL OF Materials CHEMISTRY

A multiple-quantum ^{23}Na MAS NMR study of amorphous sodium gallium silicate zeolite precursors

Sasa Antonijevic, Sharon E. Ashbrook, Richard I. Walton* and Stephen Wimperis*

School of Chemistry, University of Exeter, Stocker Road, Exeter, UK EX4 4QD. E-mail: r.i.walton@exeter.ac.uk; s.wimperis@exeter.ac.uk; Fax: +44-1392-263434

Received 8th November 2001, Accepted 12th February 2002
First published as an Advance Article on the web 19th March 2002

Amorphous sodium gallium silicate materials are isolated after short periods of heating a gel of composition Ga_2O_3 : SiO_2 : 4NaOH : 80H_2O at 100 °C. On extended heating (periods in excess of 24 hours), the crystalline zeolite gallium hydroxosodalite is produced from the reaction mixture. We have studied the materials using ^{23}Na (I = 3/2) MAS and multiple-quantum MAS (MQMAS) NMR spectroscopy in order to extract information about the local environment of the sodium in the amorphous solids, and thereby gain information about the role of sodium during the crystallisation of the zeolite. The average ^{23}Na isotropic chemical shift, δ_{iso}, and the quadrupolar parameter, $P_Q = C_Q(1 + \eta^2/3)^{1/2}$, were evaluated by analysis of the two-dimensional MQMAS spectra. In addition to the sodium gallium silicate materials, a number of crystalline sodium silicates, aluminates and gallates were also studied and their NMR parameters compared with literature values and related to crystallographic data describing the local environment of the sodium atoms. Although no simple correlation is known between ^{23}Na NMR parameters and the coordination number or average sodium–oxygen interatomic distance, a general trend of increasing δ_{iso} with decreasing coordination number and interatomic distance is apparent. The data from the amorphous sodium gallium silicates strongly suggest that even after very short periods of heating the local environment of sodium is very similar to that found in the crystalline zeolite product. Additional ^{71}Ga (I = 3/2) MAS NMR spectra were also recorded from the amorphous samples to provide information on the local gallium environment and these show the presence of tetrahedral gallium, as in the crystalline zeolite, even in the samples prepared after the shortest period of heating.

Introduction

The study of the formation mechanism of microporous silicate zeolites has recently attracted considerable attention. Both naturally-occurring and synthetic zeolites are used in a diverse range of commercial applications, in areas such as catalysis, ion-exchange and gas separation, and it is hoped that an understanding of their crystallisation mechanism will allow the development of rational syntheses of new materials for specific applications.[1,2] Several approaches have been taken in studying zeolite crystallisation mechanisms, including monitoring the reactions in real time with *in situ* probes, which include both diffraction and spectroscopic techniques,[3,4] and computer modelling of the energetics of species formed in solution prior to crystallisation.[5] Such experiments have begun to provide the first understanding of the complexities of the processes involved in the crystallisation of zeolites and other microporous materials, which usually takes place from heterogeneous mixtures under hydrothermal conditions.

In studies of the crystallisation of aluminium silicate zeolites from silica and alumina in alkali conditions, the appearance of an amorphous solid before the onset of crystallisation of the crystalline zeolite has often been observed.[6] Such material has been considered as an intermediate phase in the production of the crystalline aluminosilicate zeolite from distinct alumina and silica sources and, although isolated by quenching hydrothermal reactions to room temperature, may be structurally related to the amorphous solid observed *in situ* by small-angle scattering studies during zeolite crystallisation from clear solutions.[6] Engelhardt *et al*. studied amorphous aluminium silicates by ^{27}Al and ^{29}Si NMR spectroscopy and were able to determine that the solids were made up of a network of alternating corner-sharing AlO_4 and SiO_4 tetrahedra reminiscent of the structure of the zeolite,[7,8] and other workers have found consistent results.[9] The amorphous solids are thought of as precursors to the crystalline zeolites, and so are important to study because of their role in the crystallisation mechanism. Investigation of their structures is not easy owing to the inherent difficulties in the structural characterisation of disordered solids, and therefore the amorphous zeolite precursors remain under-characterised.

Gallium silicate zeolites have structures and properties very similar to those of the aluminium silicates, and their specific uses have been reviewed.[10] One of us recently studied a number of amorphous gallium silicates, isolated during the formation of the zeolite isostructural with hydroxosodalite, using X-ray absorption fine structure (XAFS) spectroscopy at the gallium and silicon K-edges.[11] This experiment allowed the local environments of both elements to be studied independently, and quantitative information, including bond distances and average coordination number, was obtained. Only the local environment of gallium and silicon was, however, probed in this experiment and, therefore, with the aim of further understanding the structures of the amorphous zeolite precursors, we have performed a ^{23}Na and ^{71}Ga (both I = 3/2) MAS NMR study. Although ^{71}Ga and ^{17}O MAS NMR spectra of crystalline gallium hydroxosodalite $Na_8[Ga_6Si_6O_{24}](OH)_2{\cdot}6H_2O$ have been reported by other workers,[12,13] the techniques have not yet been applied to the study of the zeolite precursors. With the advent of the two-dimensional multiple-quantum MAS NMR method,[14] it is now possible to obtain high-resolution solid-state ^{23}Na NMR spectra almost routinely and in this work we describe the use of this method to extract structural information about sodium in disordered solids.

DOI: 10.1039/b201581c

Experimental

Materials

The amorphous gallium silicates were prepared in the same manner as previously described: amorphous gallium oxide Ga_2O_3 (prepared by thermal decomposition of hydrated gallium nitrate at 220 °C overnight), fumed silica and sodium hydroxide solution were manually mixed to give an opaque mixture of composition Ga_2O_3 : SiO_2 : 4NaOH : $80H_2O$.[11] Eight identical batches were prepared using 0.25 g Ga_2O_3, and each heated separately in a 23 mL Teflon-lined hydrothermal autoclave at 100 °C for a period of 1.5, 3, 4.75, 7, 16, 19, 24 or 42 hours. After the chosen period of heating, an autoclave was removed from the oven, allowed to cool to room temperature, and the solid washed with distilled water, recovered by suction filtration and dried at 80 °C overnight. Here, we designate these samples SGS_n (sodium gallium silicate prepared after n hours of heating). Powder X-ray diffraction patterns were recorded from all of the solids using a Bruker D8 Advance diffractometer operating with CuKα radiation (average wavelength 1.5418 Å). The solids prepared after periods of heating of 24 and 42 hours are highly crystalline and all Bragg reflections could be indexed on the structure previously produced for gallium hydroxosodalite by McCusker *et al.*[15] On heating for slightly shorter periods of time (16 and 19 hours), characteristic Bragg reflections, albeit broadened, of the crystalline zeolite are present in the powder X-ray diffraction pattern, but superimposed upon a smooth background characteristic of an amorphous material. Those materials prepared after the shortest periods of heating (1.5, 3, 4.75 and 7 hours) are X-ray amorphous. Fig. 1 shows three powder X-ray diffraction patterns, representative of each type of sample.

A number of crystalline materials were used as model compounds for ^{23}Na NMR studies. Na_2SiO_3 and $Na_2SiO_2(OH)_2{\cdot}4H_2O$ were used as supplied by Alfa-Aesar. The material $NaGaO_2$ was prepared by solid-state reaction between freshly dried Na_2CO_3 and amorphous Ga_2O_3 in stoichiometric amounts at 900 °C for 32 hours. Powder X-ray diffraction was used to confirm the identities of these solids.

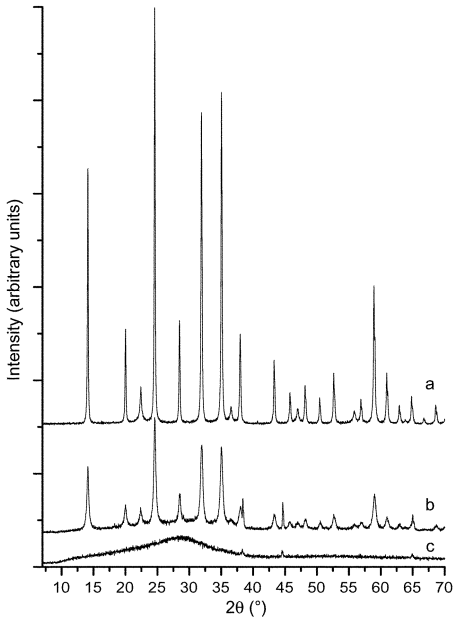

Fig. 1 Powder X-ray diffraction patterns of sodium gallium silicates prepared after (a) 24 (b) 19 and (c) 1.5 hours of reaction time. Peaks at 38°, 44° and 65° are due to the aluminium sample holder.

NMR spectroscopy

Spectra were recorded either on a Bruker MSL/Avance 400 spectrometer equipped with a widebore 9.4 T magnet, operating at a Larmor frequency, ν_0, of 105.8 MHz for ^{23}Na and 122.0 MHz for ^{71}Ga, or on a Bruker Avance 200 spectrometer equipped with a widebore 4.7 T magnet, operating at ν_0 = 52.9 MHz for ^{23}Na. All samples were packed inside 4 mm or 2.5 mm rotors and MAS rates of 9.5 kHz and 33.3 kHz, respectively, were used. Chemical shifts are reported in ppm relative to an external standard of 0.15 M NaCl (aq) for ^{23}Na and 1.0 M $Ga(NO_3)_3$ (aq) for ^{71}Ga. Two-dimensional ^{23}Na triple-quantum MAS spectra were recorded using the z-filtered sequence of Amoureux *et al.*[16]

MQMAS NMR

Solid-state NMR spectra of quadrupolar nuclei, *i.e.*, those with spin quantum number $I > \frac{1}{2}$, often exhibit low resolution owing to the presence of significant anisotropic quadrupolar broadening. This results from the interaction of the nuclear quadrupole moment (eQ) with the electric field gradient (eq). The quadrupolar interaction may be parameterized by its magnitude, $C_Q = e^2qQ/h$, and asymmetry, η, where $0 \leqslant \eta \leqslant 1$. This interaction may be very large, often of the order of megahertzs, and results in a second-order anisotropic broadening, proportional to C_Q^2/ν_0, that cannot be fully removed by MAS alone. The multiple-quantum magic angle spinning (MQMAS) NMR technique[14,17,18] offers a method of obtaining truly high-resolution spectra of half-integer (I = 3/2, 5/2, 7/2, *etc.*) quadrupolar nuclei through the removal of the second-order broadening. The technique involves two-dimensional correlation of multiple- and single-quantum coherences under MAS conditions. This results in a refocusing of the anisotropic quadrupolar broadening, whilst retaining the isotropic shifts. A two-dimensional Fourier transform yields a spectrum containing ridge-like lineshapes which lie along a gradient equal to the so-called MQMAS ratio, *e.g.*, −7/9 in a spin I = 3/2 triple-quantum MAS spectrum.[14,17,18] A high-resolution or isotropic spectrum may be obtained from a projection orthogonal to this axis. In this work, a z-filtered triple-quantum MAS pulse sequence was used,[16] the z-filter being employed in order to obtain pure phase two-dimensional lineshapes.

For amorphous or disordered solids, NMR is a valuable tool owing to its ability to probe local environment despite the lack of long range order. However, the continuum of local environments encountered in such materials leads to distributions in the isotropic chemical shifts and/or quadrupolar parameters of the nucleus studied.[19] These further broaden the spectrum and restrict the information available. The increased resolution offered by MQMAS makes it a useful technique for the study of disordered materials and, in particular, many applications of ^{11}B (I = 3/2), ^{17}O (I = 5/2), ^{23}Na (I = 3/2), and ^{27}Al (I = 5/2) MQMAS NMR in amorphous systems may be found in the literature.[17,19–25]

Results

Fig. 2 shows conventional ^{23}Na MAS NMR spectra of five of the sodium gallium silicates, recorded at B_0 field strengths of 9.4 T and 4.7 T. All spectra display a single resonance in the range δ 0–40 ppm with little indication of the lineshape features characteristic of second-order quadrupolar broadening. The spectra of $SGS_{1.5}$ and SGS_7 exhibit broad and slightly asymmetric lineshapes, typical of those observed for amorphous or disordered materials. As expected, the lineshapes at 4.7 T are significantly broader than those recorded at 9.4 T owing to the increase in the quadrupolar broadening (proportional to $1/B_0$). Compared with $SGS_{1.5}$ and SGS_7, the

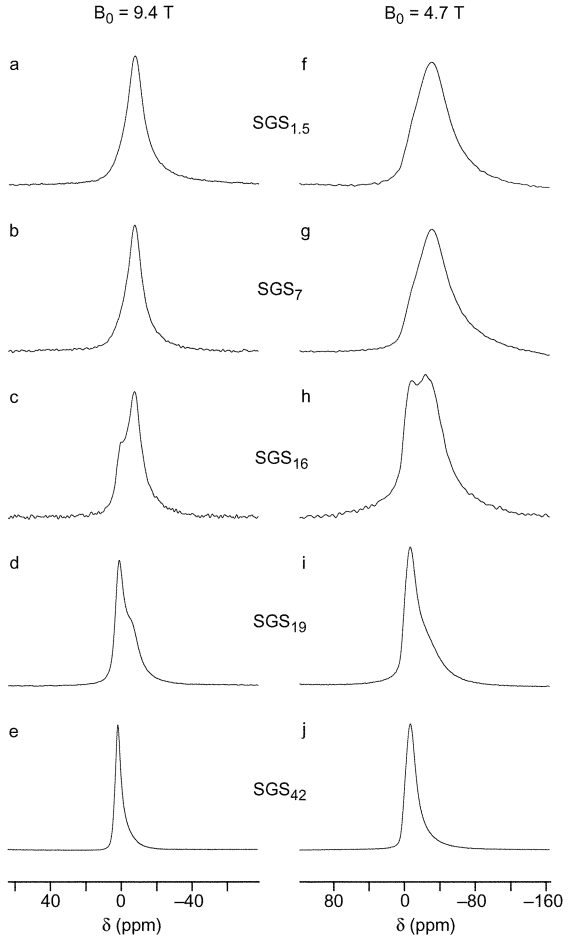

Fig. 2 ^{23}Na MAS NMR spectra of (a, f) $SGS_{1.5}$, (b, g) SGS_7, (c, h) SGS_{16}, (d, i) SGS_{19} and (e, j) SGS_{42}, recorded at (a–e) 9.4 T and (f–j) 4.7 T. In each case, the MAS rate was 9.5 kHz.

sample heated for the longest duration, SGS_{42}, displays a much narrower lineshape which, at both field strengths, is shifted slightly towards higher frequency. Interestingly, even this crystalline sample does not exhibit a typical second-order quadrupolar broadened lineshape. The spectra of SGS_{16} and SGS_{19} possess more complex resonances, apparently composed of at least two overlapping components. The additional (to the second-order quadrupolar) broadening observed in all spectra, though particularly in $SGS_{1.5}$ and SGS_7, suggests the possible presence of distributions in chemical shifts and/or quadrupolar parameters.

These trends are also reflected in the ^{71}Ga MAS NMR spectra of six of the samples shown in Fig. 3. The more crystalline samples, SGS_{24} and SGS_{42}, display a single gallium resonance (with spinning sidebands denoted by *) centred on $\delta \sim 160$ ppm. This resonance does not exhibit a lineshape characteristic of second-order quadrupolar broadening, with considerable additional broadening present. Samples heated for shorter durations display significantly broader lineshapes with more significant spinning sidebands. Although small differences in the observed chemical shift are apparent, all spectra display lineshapes with a chemical shift that is characteristic of four-coordinate gallium. Unlike for ^{23}Na, a simple correlation between ^{71}Ga isotropic chemical shift and the coordination number is quite well established[12,26,27] (*e.g.*, in β-Ga_2O_3, the four-coordinate gallium has an isotropic chemical shift, δ_{iso}, of $\sim$200 ppm, while the six-coordinate site has δ_{iso} $\sim$40 ppm[27]). For our amorphous samples, the fact that the observed shifts ($\delta \sim 140$ ppm) are typical of gallium coordinated by four atoms is particularly interesting (*e.g.*, for $SGS_{1.5}$), as even short heating durations have completely

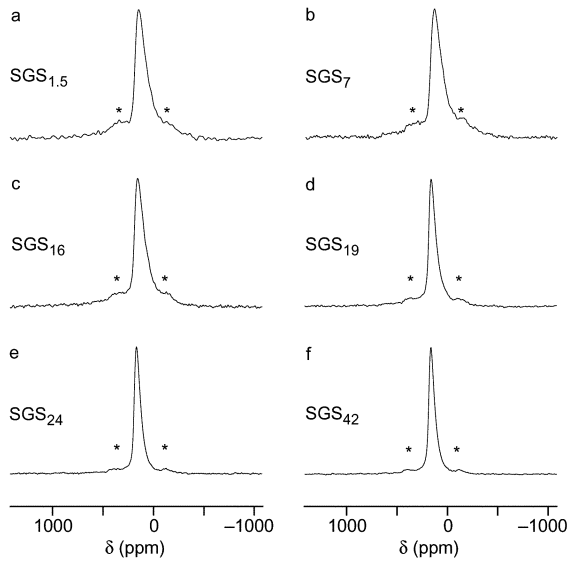

Fig. 3 ^{71}Ga MAS NMR spectra of (a) $SGS_{1.5}$, (b) SGS_7, (c) SGS_{16}, (d) SGS_{19}, (e) SGS_{24} and (f) SGS_{42}, recorded at 9.4 T. In each case, the MAS rate was 33.3 kHz. Spinning sidebands are indicated by *.

converted the six-coordinate gallium in the starting material[12] to gallium in a four-coordinate environment.

Two-dimensional triple-quantum ^{23}Na MAS NMR spectra of six of the sodium gallium silicates, recorded at $B_0 = 9.4$ T, are shown in Fig. 4. It is possible to divide these into three groups: (i) the spectra of $SGS_{1.5}$ and SGS_7 that display a single

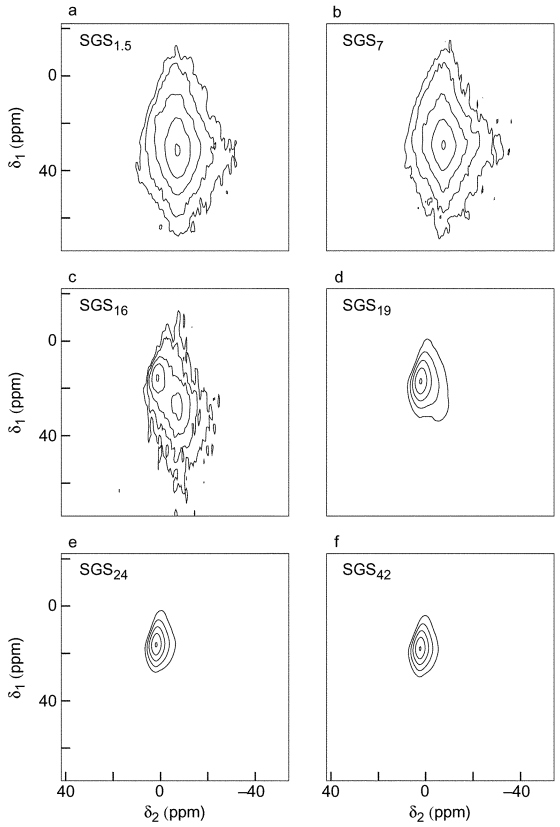

Fig. 4 Two-dimensional ^{23}Na triple-quantum MAS NMR spectra of (a) $SGS_{1.5}$, (b) SGS_7, (c) SGS_{16}, (d) SGS_{19}, (e) SGS_{24} and (f) SGS_{42}, recorded using a *z*-filtered pulse sequence at 9.4 T. In (a, b) 192, (c) 576 and (d–f) 96 transients were acquired for each of (a, b) 128, (c) 96 and (d–f) 256 t_1 increments of 10 μs. In each case, the recycle interval was 1 s and the MAS rate was 9.5 kHz. Contour levels are drawn at 6, 12, 24, 48 and 96% of the maximum value. Sign discrimination in δ_1 was achieved using time-proportional phase incrementation (TPPI).

broad resonance; (ii) those of SGS_{24} and SGS_{42} that exhibit a considerably narrower resonance; and (iii) those of SGS_{16} and SGS_{19} that appear to be a superposition of the spectra in groups (i) and (ii). With respect to group (iii) however, it should be noted that the relative proportions of the two lineshape components are very different between SGS_{16} and SGS_{19}. These qualitative observations are entirely consistent with the X-ray powder diffraction patterns of these two solids which clearly show the presence of both amorphous and crystalline components.

None of the spectra in Fig. 4 displays a ridge-like lineshape lying along a gradient equal to the MQMAS ratio (−7/9), again showing the presence, in addition to the second-order quadrupolar interaction, of other broadening mechanisms. For spin $I = 3/2$ nuclei, the presence of a distribution of quadrupolar parameters is expected to produce an isotropic second-order broadening (proportional to $1/B_0$) along an axis with a gradient of −3, whilst a distribution of isotropic chemical shifts (proportional to B_0) yields a broadening along a +3 axis in the triple-quantum MAS spectrum.[28] A qualitative inspection suggests that both additional broadening mechanisms may be present in all the spectra in Fig. 4.

Fig. 5 shows two-dimensional triple-quantum ^{23}Na MAS NMR spectra of $SGS_{1.5}$ and SGS_{42}, recorded at 4.7 T. The two-dimensional lineshapes in these spectra differ significantly from those found at 9.4 T because of the different dependence on B_0 of the second-order quadrupolar and chemical shift interactions. The position and lineshape of the narrower SGS_{42} resonance corresponds to that of a distinct "lobe" in the much broader $SGS_{1.5}$ resonance, indicating that a small amount of sodium in an environment very similar to that in the crystalline zeolite is present in the amorphous sample prepared using the shortest heating period. This observation is supported by the presence of a similar, although less distinct, salient in the 9.4 T ^{23}Na MQMAS spectra of $SGS_{1.5}$ and SGS_7 in Figs. 4a and 4b and by the presence of a shoulder on the high frequency side of the ^{23}Na MAS NMR lineshapes of $SGS_{1.5}$ and SGS_7 in Figs. 2f and 2g.

Although distributions of chemical shift and quadrupolar interactions appear to be present in the sodium gallium silicate precursors, it is possible to obtain average values of these parameters from the spectra in Figs. 4 and 5. The δ_1 and δ_2 shifts of the centre of gravity of a lineshape depend upon both the isotropic chemical shift, δ_{iso}, and the isotropic quadrupolar shift parameter, δ_Q. For spin $I = 3/2$ triple-quantum MAS spectra:[28]

$$\delta_1 = 3\delta_{iso} + \frac{6}{5}\delta_Q \quad (1)$$

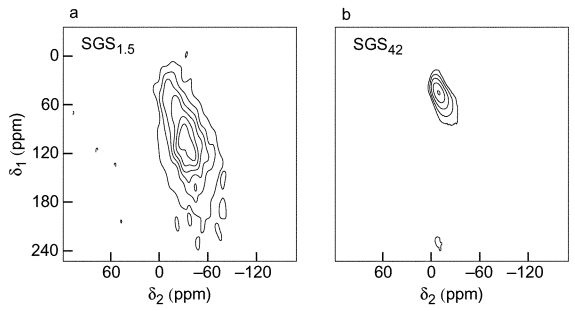

Fig. 5 Two-dimensional ^{23}Na triple-quantum MAS NMR spectra of (a) $SGS_{1.5}$ and (b) SGS_{42}, recorded using a *z*-filtered pulse sequence at 4.7 T. In (a) 960 transients were recorded for each of 128 t_1 increments of 10 μs, whilst in (b) 480 transients were recorded for each of 200 t_1 increments of 10 μs. In each case, the recycle interval was 1 s and the MAS rate was 9.5 kHz. Contour levels are drawn at (a) 15, 30, 45, 60, 75 and 90% and (b) 6, 12, 24, 48 and 96% of the maximum value. Sign discrimination in δ_1 was achieved using TPPI.

$$\delta_2 = \delta_{iso} - \frac{2}{5}\delta_Q. \quad (2)$$

Thus, from the position of the centre of gravity, both δ_{iso} and δ_Q may be determined. The quadrupolar product,[29] $P_Q = C_Q(1 + \eta^2/3)^{1/2}$, is related to δ_Q and may also be extracted. For spin $I = 3/2$:

$$P_Q = \frac{\nu_0\sqrt{\delta_Q}}{250}. \quad (3)$$

However, the individual quadrupolar parameters, C_Q and η, cannot be separated by this approach.

Table 1 gives the δ_{iso} and P_Q values obtained from the two-dimensional ^{23}Na NMR spectra of all sodium gallium silicates studied. The materials heated for a shorter duration ($SGS_{1.5}$, SGS_3, $SGS_{4.75}$ and SGS_7) have very similar average P_Q values of ~2.2 MHz, while the samples heated for much longer durations (SGS_{19}, SGS_{24} and SGS_{42}) show a significantly smaller quadrupolar interaction, with P_Q values of ~1.4 MHz. Extraction of NMR parameters from the spectrum of SGS_{16} is significantly hindered by the presence of two overlapping lineshapes. However, the positions of the highest points of the two components reveal that one is very similar to that observed in $SGS_{1.5}$, SGS_3, $SGS_{4.75}$ and SGS_7, while the other is similar to that found in SGS_{19}, SGS_{24} and SGS_{42}. Although two lineshape components may be present in samples other than SGS_{16}, their very unequal intensities do not appear to result in the position of the centre of gravity of the spectrum being significantly affected.

As mentioned above, the spectra in Figs. 4 and 5 reveal evidence of distributions in the parameters δ_{iso} and P_Q whose average values are given in Table 1. The half-width at half-height of these distributions may be estimated using a simple lineshape-fitting procedure[24] based on taking projections of the two-dimensional lineshape. The distributions in C_Q and δ_{iso} are modelled by Gaussian lineshapes, truncated at 0.02%, with η assumed to be 1. However, the presence of two components in many resonances limits the use of this method to the more crystalline samples (SGS_{24} and SGS_{42}). In these cases, half-height distributions in C_Q of ±0.1 MHz, centred on a mean value of 1 MHz, and in δ_{iso} of ±1.5 ppm centred on a mean of 3 ppm were obtained. The distributions present in the more amorphous samples are estimated to be between two and three times larger.

Relationship between sodium local environment and ^{23}Na chemical shift

In order to investigate whether ^{23}Na NMR spectra of solids can be used to derive structural information, we have compared our new experimental data with those of previous studies by other workers. We limit our discussion to materials related

Table 1 Average ^{23}Na isotropic chemical shifts (δ_{iso}, relative to 0.15 M NaCl (aq)) and quadrupolar products (P_Q) for the sodium gallium silicates extracted from centres of gravity of two-dimensional ^{23}Na MQMAS NMR lineshapes. Typical measurement errors in the values quoted are ±1.0 ppm (δ_{iso}) and ±0.3 MHz (P_Q)

Sample	δ_{iso} (ppm)	P_Q/MHz
$SGS_{1.5}$ (9.4 T)	–0.5	2.2
SGS_3 (9.4 T)	0.0	2.2
$SGS_{4.75}$ (9.4 T)	0.4	2.1
SGS_7 (9.4 T)	–0.5	2.2
SGS_{16} (9.4 T)	–	–
SGS_{19} (9.4 T)	1.7	1.4
SGS_{24} (9.4 T)	1.8	1.4
SGS_{42} (9.4 T)	2.6	1.4
$SGS_{1.5}$ (4.7 T)	1.0	1.9
SGS_{42} (4.7 T)	1.4	1.3

Table 2 Coordination numbers, mean Na–O bond distances (<Na–O>) and isotropic ^{23}Na chemical shifts (δ_{iso}, relative to 0.15 M NaCl (aq)) for model silicate compounds taken from both this work ([a]) and the literature

Compound	Coordination number	<Na–O>/Å	Refs.	δ_{iso} (ppm)	Refs.
$NaAlO_2$	4	2.350	38	26.2	42
$NaGaO_2$	4	2.323	39	27.0	[a]
Na_2SiO_3	5	2.342	30	22.7	42, [a]
$Na_2SiO_2(OH)_2{\cdot}4H_2O$	5	2.397	31	9.0	42, [a]
	5	2.350		9.5	
α-$Na_2Si_2O_5$	5	2.397	32	24.6	42
NaOH	5	2.405	40	19.4	42
$Na_2Si_4O_8(OH)_2(H_2O)_4$ (makatite)	5	2.396	33	8.0	45
	6	2.491		0.0 or 1.0	
	6	2.459		0.0 or 1.0	
β-$Na_2Si_2O_5$	5	2.418	41	27.6	42
	6	2.454		15.5	
$Na_2SiO_2(OH)_2{\cdot}8H_2O$	6	2.459	34	3.5	42
$NaAlSi_2O_6$	6	2.402	37	11.0	46
$Na_8[Ga_6Si_6O_{24}](OH)_2{\cdot}6H_2O$ (Ga-sodalite)	6	2.452	15	2.0	[a]
$Na_2SiO_2(OH)_2{\cdot}7H_2O$	6	2.473	35	6.3	42
	6	2.420		6.5	
$Na_2SiO_2(OH)_2{\cdot}5H_2O$	6	2.428	36	5.7	42
	6	2.519		0.0	

[a]Values from this work.

chemically to our sodium gallium silicate samples: sodium silicates, sodium aluminium silicates, sodium aluminates and sodium gallates.[30–41] A number of workers have studied a range of crystalline and glassy sodium silicates using ^{23}Na NMR spectroscopy and some have attempted to establish a correlation between the isotropic chemical shift, δ_{iso}, and the local atomic arrangement of atoms about sodium (bond distances, coordination number and geometry). For example, Koller *et al.*[42] derived a "shift parameter", *A*, for a number of crystalline sodium-containing materials by considering the bond valence parameter of each bond to sodium and each individual bond length. These workers then established an empirical relationship between *A* and δ_{iso}, although, in order to achieve a linear correlation, the shift parameter had to be defined by weighting the bond distances by an exponent. Stebbins reported a linear correlation between mean Na–O distance and δ_{iso} in a series of anhydrous silicates and noted that for sites with higher coordination numbers the chemical shift is significantly lower.[43] Angeli *et al.* have used this qualitative relationship in combination with molecular dynamics simulations to predict Na–O bond distances in sodium silicate glasses.[44] It is apparent that a relationship exists between sodium local environment and the isotropic ^{23}Na chemical shift, but that interpretation is not unambiguous or necessarily straightforward.

Table 2 contains ^{23}Na NMR parameters for a number of materials relevant to our discussion;[42,45,46] included are the new data we have measured and other previously determined values. Also shown are crystallographic parameters relating to the average local environment of sodium in each of the compounds.[30-41] In each material, the first coordination shell of sodium consists of between four and six oxygen atoms at mean distances between 2.32 and 2.52 Å. The type of atom in the second coordination shell of sodium varies for each compound, but it can be seen that this has little effect on the magnitude of δ_{iso}. For example, for $NaAlO_2$ and $NaGaO_2$, which are isostructural, differing only very slightly in Al–O and Ga–O interatomic distances,[38,39] the ^{23}Na chemical shift is similar and significantly larger than observed in the other materials.[42] In Fig. 6, δ_{iso} is plotted against mean Na–O interatomic distance, using the data given in Table 2, with the coordination numbers of each sodium site highlighted. It is apparent that there exists a general trend of increasing chemical shift with decreasing coordination number and interatomic distance. The fact that coordination number and interatomic distance should be closely related is not unexpected: for steric reasons, it is commonly observed that a smaller number of coordinating atoms will reside at a smaller distance from the central atom.

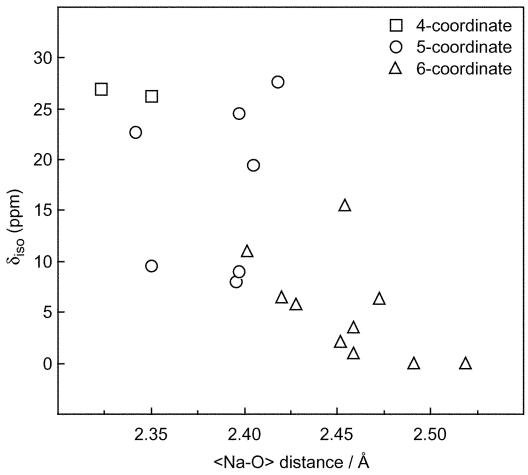

Fig. 6 ^{23}Na isotropic chemical shifts, δ_{iso}, plotted against mean Na–O bond distances for a range of model compounds, as shown in Table 2. Squares, circles and triangles denote four-, five- and six-coordinate sodium, respectively.

Discussion and conclusions

The primary aim of our study was to compare the ^{23}Na δ_{iso} values obtained for the amorphous sodium gallium silicates with those from the crystalline model compounds in order to infer structural information about the disordered solids. Although the chemical shift range of ^{23}Na is rather small compared with those of other nuclides (notably ^{27}Al or ^{71}Ga), there is a distinct dependence of chemical shift on local atomic environment of sodium. The amorphous precursor materials all exhibit isotropic chemical shift values of $\sim$0 ppm, which are comparable to those seen in the crystalline zeolite product and significantly smaller than those typically seen in materials where the coordination number is lower than six and/or the interatomic separation is shorter than 2.4 Å. We can therefore conclude from this study that the local environment of sodium in the amorphous materials closely resembles that in the final crystalline zeolite product. This is comparable with the previous XAFS study[11] of the local environment of Si and Ga in the amorphous materials which revealed that both

elements are found in tetrahedral units, linked in an alternating manner, in the same way as in the zeolite. Clearly, the amorphous solid resembles the crystalline zeolite in terms of local atomic structure, even after very short periods of heating. Further evidence for this is provided by the ^{71}Ga MAS spectra, which showed that even after a very short heating period ($\sim$1.5 hours) the six-coordinate gallium in the starting material had been fully converted to gallium in a four-coordinate environment.

It is noteworthy that the ^{23}Na spectra of X-ray amorphous samples prepared with short heating time exhibit salients in the two-dimensional lineshapes that suggest the presence of two types of sodium: one characteristic of the crystalline zeolite product, and the other due to a disordered phase. In the samples prepared with longer heating durations, the amount of crystalline component increases and, for the materials shown by powder X-ray diffraction to consist of distinct amorphous and crystalline components, the presence of two sodium environments is clearly seen. The presence of some local order resembling the crystalline zeolite, even after very short reaction times, is consistent with currently accepted models for zeolite crystal growth, in particular that nucleation sites, essentially nanometer-sized zeolite building blocks, form in the precursor gel and act as centres for crystal growth.[6] Previous electron microscopy studies have revealed the presence of such nanoparticles, for example, in the synthesis of the aluminosilicate zeolite Y.[47] NMR is thus able to probe local order on a length-scale smaller than possible by X-ray diffraction and reveals regions of local order in amorphous materials.

We have provided further evidence for a correlation between ^{23}Na chemical shift and the average local environment of sodium in the solid state, as previously suggested by other workers.[42–44] Although the chemical shift range is not as marked as for other elements which are routinely studied by NMR, the relationship potentially has great use in identifying the local atomic arrangement of sodium in amorphous materials or in aiding structural characterisation of new crystalline materials. The origin of the effect of the correlation between chemical shift and Na–O bond distance and coordination number is worthy of greater study, and this will be the subject of future research.

Acknowledgement

We thank EPSRC for generous support (grant no. GR/N07622).

References

1 M. E. Davis, *Stud. Surf. Sci. Catal.*, 1995, **97**, 35.
2 R. J. Francis and D. O'Hare, *J. Chem. Soc., Dalton Trans.*, 1998, 3133.
3 A. K. Cheetham and C. Mellot, *Chem. Mater.*, 1997, **9**, 2269.
4 R. I. Walton and D. O'Hare, *Chem. Commun.*, 2000, 2283.
5 C. R. A. Catlow, D. S. Coombes and J. C. G. Pereira, *Chem. Mater.*, 1998, **10**, 3249.
6 D. P. Serrano and R. van Grieken, *J. Mater. Chem.*, 2001, **11**, 2391.
7 G. Engelhardt, B. Fahlke, M. Magi and E. Lippmaa, *Zeolites*, 1983, **3**, 292.
8 G. Engelhardt, B. Fahlke, M. Magi and E. Lippmaa, *Zeolites*, 1985, **5**, 49.
9 I. I. Ivanova, R. Aiello, J. B. Nagy, F. Crea, E. G. Derouane, N. Dumont, A. Nastro, B. Subotic and F. Testa, *Microporous Mater.*, 1994, **3**, 245.
10 R. Fricke, H. Kosslick, G. Lischke and M. Richter, *Chem. Rev.*, 2000, **100**, 2303.
11 R. I. Walton and D. O'Hare, *J. Phys. Chem. Solids*, 2001, **62**, 1469.
12 H. K. C. Timken and E. Oldfield, *J. Am. Chem. Soc.*, 1987, **109**, 7669.
13 H. K. C. Timken, N. Janes, G. L. Turner, S. L. Lambert, L. B. Welsh and E. Oldfield, *J. Am. Chem. Soc.*, 1986, **108**, 7236.
14 L. Frydman and J. S. Harwood, *J. Am. Chem. Soc.*, 1995, **117**, 5367.
15 L. B. McCusker, W. M. Meier, K. Suzuki and S. Shin, *Zeolites*, 1986, **6**, 388.
16 J. P. Amoureux, C. Fernandez and S. Steuernagel, *J. Magn. Reson. A*, 1996, **123**, 116.
17 C. Fernandez and J. P. Amoureux, *Solid State Nucl. Magn. Reson.*, 1996, **5**, 315.
18 S. P. Brown and S. Wimperis, *J. Magn. Reson.*, 1997, **128**, 42.
19 A. P. M. Kentgens, *Geoderma*, 1997, **80**, 271.
20 S. J. Hwang, C. Fernandez, J. P. Amoureux, J. W. Han, J. Cho, S. W. Martin and M. Pruski, *J. Am. Chem. Soc.*, 1998, **120**, 7337.
21 J. F. Stebbins, J. V. Oglesby and Z. Xu, *Am. Mineral.*, 1997, **82**, 1116.
22 M. Hunger, P. Sarv and A. Samoson, *Solid State Nucl. Magn. Reson.*, 1997, **9**, 115.
23 F. Angeli, T. Charpentier, P. Faucon and J. C. Petit, *J. Phys. Chem. B*, 1999, **103**, 10356.
24 J. McManus, S. E. Ashbrook, K. J. D. MacKenzie and S. Wimperis, *J. Non-Cryst. Solids*, 2001, **282**, 278.
25 S. E. Ashbrook, J. McManus, K. J. D. MacKenzie and S. Wimperis, *J. Phys. Chem. B*, 2000, **104**, 6408.
26 A. P. M. Kentgens, C. R. Bayense, J. H. C. van Hooff, J. W. de Haan and L. J. M. van de Ven, *Chem. Phys. Lett.*, 1991, **176**, 399.
27 D. Massiot, I. Farnan, N. Gautier, D. Trumeau, A. Trokiner and J. P. Coutures, *Solid State Nucl. Magn. Reson.*, 1995, **4**, 241.
28 P. R. Bodart, *J. Magn. Reson.*, 1998, **133**, 207.
29 K. T. Mueller, J. H. Baltisberger, E. W. Wooten and A. Pines, *J. Phys. Chem.*, 1992, **96**, 7001.
30 F. Liu, S. H. Garofalini, R. D. King-Smith and D. Vanderbilt, *Chem. Phys. Lett.*, 1993, **215**, 401.
31 R. L. Schmid, J. Felsche and G. J. McIntyre, *Acta. Crystallogr. Sect. C: Cryst. Struct. Commun.*, 1985, **41**, 638.
32 A. K. Pant and D. W. J. Cruickshank, *Acta. Crystallogr. Sect. B: Struct. Crystallogr. Cryst. Chem.*, 1968, **24**, 13.
33 H. Annehed, L. Falth and F. J. Lincoln, *Z. Kristallogr.*, 1982, **159**, 203.
34 P. B. Jamieson and L. S. Dent-Glasser, *Acta. Crystallogr.*, 1966, **20**, 688.
35 J. Felsche, B. Ketterer, R. L. Schmid and D. Gregson, *Acta. Crystallogr. Sect. C: Cryst. Struct. Commun.*, 1987, **43**, 1015.
36 P. P. Williams and L. S. Dent-Glasser, *Acta. Crystallogr. Sect. B: Struct. Crystallogr. Cryst. Chem.*, 1971, **27**, 2269.
37 C. T. Prewitt and C. W. Burnham, *Am. Mineral.*, 1966, **51**, 956.
38 J. A. Kaduk and S. Y. Pei, *J. Solid State Chem.*, 1995, **115**, 126.
39 H. P. Müller and R. Hoppe, *Z. Anorg. Allg. Chem.*, 1992, **611**, 73.
40 H. Jacobs, J. Kockelkorn and T. Tacke, *Z. Anorg. Allg. Chem.*, 1985, **531**, 119.
41 A. K. Pant, *Acta. Crystallogr. Sect. B: Struct. Crystallogr. Cryst. Chem.*, 1968, **24**, 1077.
42 H. Koller, G. Englehardt, A. P. M. Kentgens and J. Sauer, *J. Phys. Chem.*, 1994, **98**, 1544.
43 J. F. Stebbins, *Solid State Ionics*, 1998, **112**, 137.
44 F. Angeli, J. M. Delaye, T. Charpentier, J. C. Petit, D. Ghaleb and P. Faucon, *J. Non-Cryst. Solids*, 2000, **276**, 132.
45 M. Hanaya and R. K. Harris, *Solid State Nucl. Magn. Reson.*, 1997, **8**, 147.
46 X. Y. Xue and J. F. Stebbins, *Phys. Chem. Minerals*, 1993, **20**, 297.
47 S. Mintova, N. H. Olson and T. Bein, *Angew. Chem., Int. Ed.*, 1999, **38**, 3202.